

Transport properties of random media: An energy-density CPA approach

K. Busch

*Ames Laboratory and Department of Physics and Astronomy, Iowa State University, Ames, Iowa 50011
and Institut für Theorie der Kondensierten Materie, Universität Karlsruhe, 76128, Karlsruhe, Germany*

C. M. Soukoulis

Ames Laboratory and Department of Physics and Astronomy, Iowa State University, Ames, Iowa 50011

(Received 1 November 1995)

We present an approach for efficient, accurate calculations of the transport properties of random media. It is based on the principle that the wave energy density should be uniform when averaged over length scales larger than the size of the scatterers. This method captures the effects of the resonant scattering of the individual scatterer exactly, and by using a coated sphere as the basic scattering unit, multiple scattering contributions may be incorporated in a mean-field sense. Its application to both “scalar” and “vector” classical waves gives exact results in the long-wavelength limit as well as excellent agreement with experiment for the mean free path, transport velocity, and the diffusion coefficient for finite frequencies. Furthermore, it qualitatively and quantitatively agrees with experiment for all densities of scatterers and contains no adjustable parameter. This approach is of general use and can be easily extended to treat different types of wave propagation in random media. [S0163-1829(96)05626-3]

I. INTRODUCTION

The study of waves propagating in strongly scattering random media is a subject with a long and rich history. However, until recently the interest of the physics community was primarily focusing on quantum, i.e., electronic, waves. It was the observation of the coherent backscattering effect in classical wave systems,¹ the analogous effect to weak localization in the electronic case, which triggered a burst of interest in further studies of strongly scattering disordered classical wave systems.¹ Although the analogy between quantum and classical waves works reasonably well, the localization of classical waves has not been observed as yet, despite the fact that recent experimental results² reported very low values for the diffusion coefficient D . In fact, it was already realized in the work of van Albada *et al.*² that, unlike electronic systems, there exists another renormalization mechanism of the diffusion coefficient D in classical wave systems. Using a scalar Bethe-Salpeter equation in the low-density regime, van Albada *et al.*² were able to show that the presence of resonant scatterers may cause the transport velocity v_E to decrease sharply close to the single-scatterer resonances. This renormalization of the diffusion coefficient D (Refs. 3–9) can be viewed as either being the result of a different Ward Identity due to an energy-dependent scattering potential or being caused by a scattering delay due to the storage of wave energy inside a single scatterer. Therefore, considerable care has to be exerted when interpreting low values of the diffusion coefficient $D = v_E \ell_t / 3$, since only low values of the transport mean free path ℓ_t signify localization. To further extend their results to the vector case, van Albada *et al.* simply replaced the single-scatterer t matrix with the vector t matrix. However, this is an oversimplified approximation to the real vector problem. The polarizations of the electromagnetic (EM) waves have to be taken into account in a fully vector calculation in deriving the Boltzmann equation,

starting from the Bethe-Salpeter equation. In addition, experimental results⁹ for alumina spheres have shown that as the volume fraction of the scatterers, f , increases towards close packing ($f \approx 0.60$), there is no structure in the diffusion coefficient versus frequency. This clearly suggests that there is no structure in the transport velocity. This behavior is not observed when extending the low-density theory of van Albada *et al.* to this high- f regime. It is by now well understood that to lowest order in the density of the dielectric scatterers, the strong decrease in the transport velocity is due to the (single-scatterer) Mie resonances. For higher values of the density, multiple scattering corrections become appreciable and tend to wash out the single-scatterer resonances, as observed experimentally.

In the spirit of the coherent-potential approximation (CPA) a conceptually different approach to the problem of classical wave propagation in strongly scattering random media was recently developed¹⁰ and obtained a CPA velocity for $f = 0.60$, which is qualitatively consistent with experiment, in not showing any structure as a function of the frequency. Not surprisingly, the newly developed¹⁰ coated CPA for low f gives a CPA velocity which reduces to the regular phase velocity which is higher than the velocity of light near Mie resonances. This is an undesirable feature of the CPA which can be understood to be the result of underestimating the above-mentioned energy-storage effect. Thus, for small f , the theory of van Albada *et al.*² seems to give the correct transport velocity v_E , while for large f , it is the coated CPA approach^{10,11} which seems to give transport properties consistent with experiment.⁹

In the present paper, we report the details of an approach¹² for calculating the transport properties of random media that takes into account the multiscattering effects in a mean-field sense. It can be applied to all cases of classical wave propagation in random media, such as acoustic (scalar), EM (vector), and elastic (tensor) waves. Furthermore, this

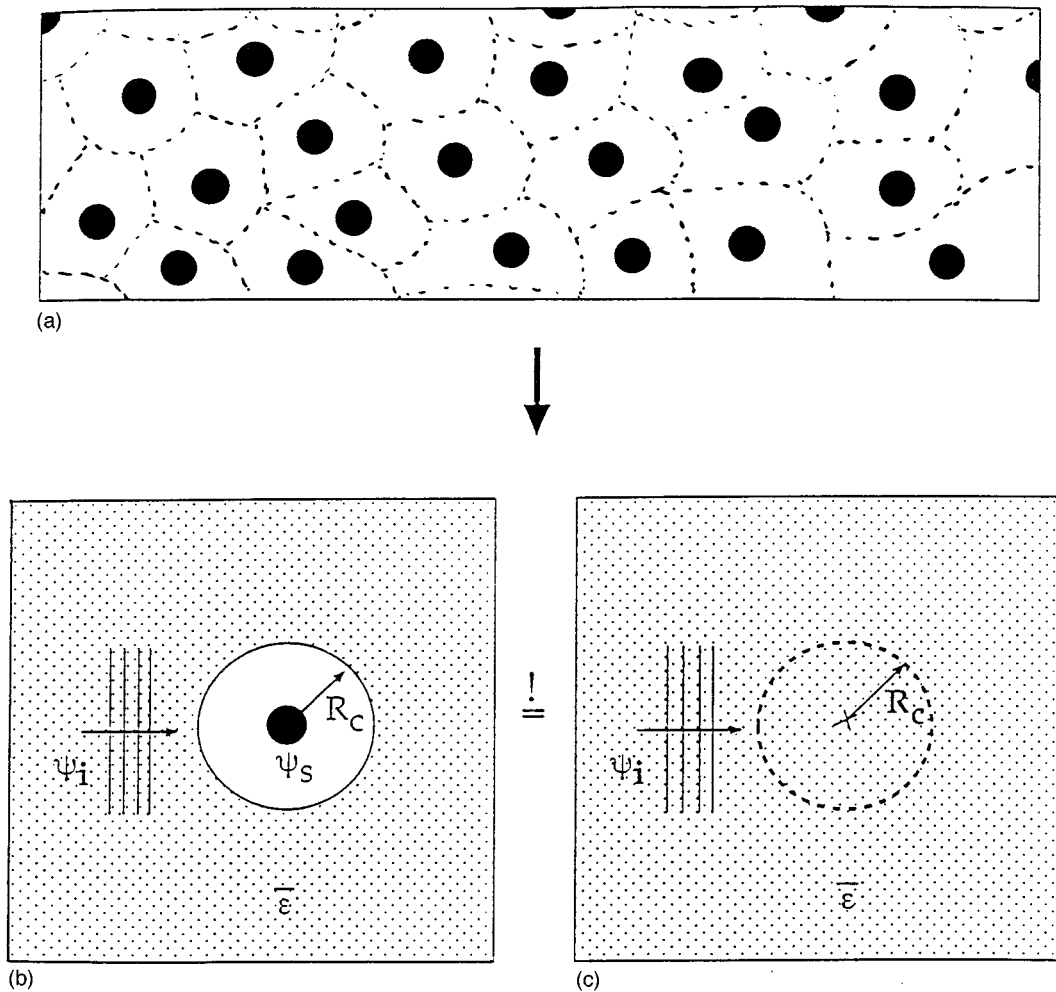


FIG. 1. (a) In a random medium composed of dielectric spheres, the basic scattering unit may be regarded as a coated sphere, as represented by the dashed lines. To calculate the effective dielectric constant $\bar{\epsilon}$, a coated sphere of radius $R_c = R/f^{1/3}$, is embedded in a uniform medium. The self-consistent condition for the determination of $\bar{\epsilon}$ is that the energy of a coated sphere (b) is equal to the energy of a sphere with radius R_c and dielectric constant $\bar{\epsilon}$ (c).

approach gives results which are in qualitative agreement with experiment for *all* densities of scatterers. The paper is organized as follows. In Sec. II we give a detailed description of our general method for scalar and vector waves, emphasizing the conceptual difference from the conventional CPA. For the long-wavelength limit, analytical results are presented in Sec. III, whereas the numerical results for finite frequencies are discussed in Sec. IV. Finally, Sec. V is devoted to a discussion of the results.

II. MODEL AND METHOD OF CALCULATION

We consider a composite medium of two lossless materials, with dielectric constants ϵ_1 and ϵ_2 . Our medium is assumed to consist of spheres with diameter $d = 2R$ and dielectric constant ϵ_1 randomly placed within the host material with dielectric constant ϵ_2 . The random medium is characterized also by f , the volume fraction occupied by the spheres. The basic idea of effective medium theory is to focus on one particular scatterer and to replace the surrounding random medium by an effective homogeneous medium. The effective medium is determined self-consistently by taking into account the fact that any other scatterer could have

been chosen. This procedure manifests the homogeneity of the random medium on average. In conventional effective medium theories, such as the CPA, the effective medium is determined by demanding that the total cross section (TCS) of the difference between scattering medium and the effective medium vanishes on average.¹³ In the effective medium the energy density is homogeneous by construction.

However, the position of a sphere in the medium is completely random, with the exception that the spheres cannot overlap. This implies that the distribution of spacings between neighboring spheres is peaked at a distance $R_c > R$. Therefore, we may consider a coated sphere as the basic scattering unit¹⁴ (cf. Fig. 1). The radius R_c of the coated sphere is $R_c = R/f^{1/3}$. The dielectric constants of the core and the coat are ϵ_1 and ϵ_2 , respectively. This procedure also incorporates some of the multiple scattering effects at different centers. With this technique it is, therefore, possible to obtain reliable information about transport properties for the whole range of disorder, as has been demonstrated in recent works.^{10,11,15}

The use of a coated sphere as the basic scattering unit also implies that the homogeneity of the energy density is not

anymore trivially fulfilled. If we, nevertheless, apply the ideas of the conventional CPA to this new structural unit we obtain excellent agreement with experiments for quantities not directly related to the energy density, i.e., for scattering and transport mean free path.^{10,11} In contrast, quantities describing energy transport, i.e., the energy transport velocity and diffusion coefficient, show good agreement with experiment for small coating, i.e., for high disorder, but are problematic for small disorder as they give unphysical results close to the single-scatterer Mie resonances, although still being qualitatively correct. In addition, the computational effort turns out to be quite formidable due to serious convergence problems.

This unphysical behavior may be directly attributed to an inhomogeneous energy density, especially for large coating, i.e., small disorder. In the present approach we, therefore, explicitly choose the averaged energy density homogeneity as the criterion for the effective medium. Since we are exclusively considering lossless dielectrics, our effective medium dielectric constant has to be real due to energy conservation. This is in contrast to the conventional approaches and, consequently, we have to proceed in two steps: First, we determine for every frequency ω the real effective dielectric constant $\bar{\epsilon}$ by demanding the *energy density to be homogeneous on scales larger than the basic scattering unit*. Then, in a second step, the physical quantities are calculated from the (nonvanishing) scattering cross section of the resulting arrangement of coated sphere and effective medium.

Since in the above-mentioned arrangement the effective medium dielectric constant is real and the energy density is homogenous on scales larger than the basic scattering unit, the energy transport velocity v_E may now be identified with the phase velocity v_p . v_p , in turn, is determined by the TCS of the above-mentioned arrangement. In fact, for the scalar case our results for v_E agree remarkably well with the results of a similar spirited approach by Jing *et al.*¹⁴ However, our approach can just as easily treat the vector case for which even a low-density solution of the corresponding vector-Bethe-Salpeter equation is absent to date.

The requirement that the energy content of a coated sphere embedded in the effective medium and being hit by a plane wave should be the same as the energy stored by a plane wave in the same volume of the effective medium can be formulated quantitatively by the self-consistency equation

$$\int_0^{R_c} d^3r \rho_E^{(1)}(\vec{r}) = \int_0^{R_c} d^3r \rho_E^{(2)}(\vec{r}), \quad (1)$$

where $\rho_E^{(1)}(\vec{r})$ and $\rho_E^{(2)}(\vec{r})$ are the energy densities for the coated sphere and the plane wave, respectively. Clearly, this very general principle can be applied to any kind of classical wave propagation. We chose to discuss two, for practical applications very important, cases, i.e., scalar (acoustic) and vector (EM) classical waves. For a general scalar wave field $\psi(\vec{r})$ the energy density is

$$\rho_E(\vec{r}) = \frac{1}{2} [\omega^2 \epsilon(\vec{r}) |\psi(\vec{r})|^2 / c^2 + |\vec{\nabla} \psi(\vec{r})|^2], \quad (2)$$

whereas the energy density of vector waves with electric and magnetic fields $\vec{E}(\vec{r})$ and $\vec{H}(\vec{r})$ is given by

$$\rho_E(\vec{r}) = \frac{1}{2} [\epsilon(\vec{r}) |\vec{E}(\vec{r})|^2 + \mu |\vec{H}(\vec{r})|^2], \quad (3)$$

where μ is the magnetic permeability which is taken to be the same in both materials. Consequently, Eq. (1) together with either Eq. (2) or Eq. (3) determines the (real) dielectric constant $\bar{\epsilon}$ of the effective medium for every frequency. As mentioned above the energy transport velocity v_E is identified with the so-called phase velocity v_p (Ref. 14) and the scattering mean free path ℓ_s can be calculated via¹⁴

$$v_E \approx v_p = \frac{c}{\sqrt{\bar{\epsilon}}} \sqrt{1 - \text{Re}(\Sigma) / \bar{k}^2}, \quad (4)$$

$$\ell_s = \frac{1}{\sqrt{2} \text{Im}(\Sigma)} \{ [\bar{k}^2 - \text{Re}(\Sigma)] + \sqrt{[\bar{k}^2 - \text{Re}(\Sigma)]^2 + [\text{Im}(\Sigma)]^2} \}^{1/2}, \quad (5)$$

where $\bar{k} = \sqrt{\bar{\epsilon}} \omega / c$. $\text{Re}(\Sigma)$ and $\text{Im}(\Sigma)$ denote the real and imaginary parts of the self-energy Σ , respectively. In the independent scatterer approximation the self-energy Σ is given by

$$\Sigma = 4 \pi n f(0). \quad (6)$$

Here, $f(0)$ denotes the forward scattering amplitude for a coated sphere embedded in the effective medium and $n = 1/R_c^3$ is the density of scatterers. For scalar waves we have

$$f(0) = - \frac{i}{k} \sum_{l=0}^{\infty} (2l+1) D_l, \quad (7)$$

whereas for vector waves it is

$$f(0) = - \frac{i}{2k} \sum_{l=1}^{\infty} (2l+1) (A_l + B_l). \quad (8)$$

The scattering coefficients D_l , A_l , and B_l for a coated sphere are given in Ref. 14 for scalar (D_l) and in Ref. 16 for vector waves (A_l and B_l). Since the right-hand side of Eq. (1) is trivial, it is the left-hand side which causes most of the computational difficulties. Fortunately, the analytical calculations can be carried quite far. In the scalar case, using the expressions given in Ref. 14 for the scattered wave field, we find, after a good deal of cumbersome algebra, that the energy content $E^{(s)}$ of the coated sphere, i.e., the left-hand side of Eq. (1), is given by the set of equations

$$E^{(s)} = E_1^{(s)} + E_2^{(s)},$$

$$E_1^{(s)} = \frac{1}{2} \frac{\omega^2}{c^2} \epsilon_1 \sum_{l=0}^{\infty} |a_l|^2 \frac{1}{k_1^3} \int_0^{k_1 R} \rho^2 d\rho W_l^{(s)}(j_l, j_l; \rho),$$

$$E_2^{(s)} = \frac{1}{2} \frac{\omega^2}{c^2} \epsilon_2 \sum_{l=0}^{\infty} |a_l|^2 \frac{1}{k_2^3} \int_{k_2 R}^{k_2 R_c} \rho^2 d\rho \\ \times [\phi_l^2 W_l^{(s)}(j_l, j_l; \rho) + \zeta_l^2 W_l^{(s)}(n_l, n_l; \rho) \\ + 2 \phi_l \zeta_l W_l^{(s)}(j_l, n_l; \rho)],$$

$$W_l^{(s)}(z_l, \bar{z}_l; \rho) = (2l+1)z_l(\rho)\bar{z}_l(\rho) + lz_{l-1}(\rho)\bar{z}_{l-1}(\rho) \\ + (l+1)z_{l+1}(\rho)\bar{z}_{l+1}(\rho),$$

$$\phi_l = (k_2 R)^{1/2} [j_l(k_1 R)n'_l(k_2 R) - (k_1/k_2)j'_l(k_1 R)n_l(k_2 R)],$$

$$\zeta_l = (k_2 R)^{1/2} [(k_1/k_2)j_l(k_2 R)j'_l(k_1 R) - j'_l(k_2 R)j_l(k_1 R)],$$

where $k_i = \sqrt{\epsilon_i} \omega / c$ and $i = 1, 2$. j_l and n_l denote the spherical Bessel functions of first and second kinds, respectively. The a_l are the scattering coefficients for the field inside the core. Similarly, for the vector case we use the expressions in Ref. 16 and obtain for the left-hand side of Eq. (1), i.e., the energy content $E^{(v)}$ of the coated sphere,

$$E^{(v)} = E_1^{(v)} + E_2^{(v)},$$

$$E_1^{(v)} = \frac{1}{2} \frac{\omega^2}{c^2} \epsilon_1 \sum_{l=1}^{\infty} (|c_l|^2 + |d_l|^2) \frac{1}{k_1^3} \int_0^{k_1 R} \rho^2 d\rho W_l^{(v)}(j_l, j_l; \rho),$$

$$E_2^{(v)} = \frac{1}{2} \frac{\omega^2}{c^2} \epsilon_2 \sum_{l=1}^{\infty} \frac{1}{k_2^3} \int_{k_2 R_c}^{k_2 R} \rho^2 d\rho \\ \times [(|c_l|^2 \phi_l^2 + |d_l|^2 \gamma_l^2) W_l^{(v)}(j_l, j_l; \rho) \\ + (|c_l|^2 \zeta_l^2 + |d_l|^2 \eta_l^2) W_l^{(v)}(n_l, n_l; \rho) \\ + 2(|c_l|^2 \phi_l \zeta_l + |d_l|^2 \gamma_l \eta_l) W_l^{(v)}(j_l, n_l; \rho)],$$

$$W_l^{(v)}(z_l, \bar{z}_l; \rho) = (2l+1)z_l(\rho)\bar{z}_l(\rho) + (l+1)z_{l-1}(\rho)\bar{z}_{l-1}(\rho) \\ + lz_{l+1}(\rho)\bar{z}_{l+1}(\rho),$$

$$\phi_l = \psi_l(k_1 R)\chi'_l(k_2 R) - (k_2/k_1)\psi'_l(k_1 R)\chi_l(k_2 R),$$

$$\zeta_l = \psi_l(k_2 R)\psi'_l(k_1 R) - (k_2/k_1)\psi'_l(k_2 R)\psi_l(k_1 R),$$

$$\gamma_l = (k_2/k_1)\chi_l(k_2 R)\psi'_l(k_1 R) - \chi'_l(k_2 R)\psi_l(k_1 R),$$

$$\eta_l = (k_2/k_1)\psi_l(k_2 R)\psi'_l(k_1 R) - \psi'_l(k_2 R)\psi_l(k_1 R),$$

where, again, $k_i = \sqrt{\epsilon_i} \omega / c$ and $i = 1, 2$. ψ and χ denote the Ricatti-Bessel functions of first and second kinds, respectively. The c_l and d_l are the scattering coefficients for the field inside the core. We want to point out that the scattering coefficients depend on the (real) dielectric constant $\bar{\epsilon}$ of the effective medium. They can be numerically evaluated in a way similar as described in Ref. 16. In addition, we want to stress the great similarity between the expressions for scalar and vector waves. The only differences are that—in contrast to scalar waves—the vector waves do not have an s -wave, i.e., $l=0$, component, whereas the vector wave has two polarizations (reflected by the two scattering coefficients c_l and d_l). Finally, the expressions for $W_l^{(s)}$ and $W_l^{(v)}$ differ in a very characteristic way.

III. LONG-WAVELENGTH LIMIT

If a wave with wavelength much larger than the scatterer size and mean scatterer spacing propagates through a random medium, it cannot resolve the disorder and, therefore, we may define a frequency-independent, long-wavelength di-

electric constant ϵ_∞ according to

$$\epsilon_\infty = \lim_{\omega \rightarrow 0} \left(\frac{c}{v_E(\omega)} \right)^2. \quad (9)$$

The history of long-wavelength dielectric constants itself is an old but, nevertheless, still very active field. To name but a few, we mention the classic theories of Bruggeman¹⁷ and Maxwell-Garnett,¹⁸ and the more modern works of Bergman,¹⁹ who showed that the classic theories follow from a more general expression by making special choices for the so-called Bergman spectral function. For the topology of our model system, i.e., spheres of dielectric constant ϵ_1 embedded in a medium with dielectric constant ϵ_2 and a filling fraction f of the spheres, it is well known¹⁶ that in the scalar case the correct result for ϵ_∞ is given by the volume-averaged dielectric constant, whereas in the vector case it is Maxwell-Garnett theory which gives the right answer. To calculate ϵ_∞ according to Eq. (9) we have to proceed in two steps. First, we need to calculate $\bar{\epsilon}$ for $\omega \rightarrow 0$ from Eq. (1) and use this result to obtain an expression for $v_E(\omega)$ as $\omega \rightarrow 0$. In the scalar case, a careful analysis of Eq. (1) reveals that the leading contribution as $\omega \rightarrow 0$ comes from the $l=0$ terms. If we abbreviate the right-hand side of Eq. (1) by $\bar{E}^{(s)}$ we find for the relevant quantities

$$a_0 \approx 1 + O(\omega),$$

$$D_0 \approx -\frac{1}{3} i \frac{\omega^3}{c^3} \sqrt{\bar{\epsilon}} \left[(\epsilon_2 - \bar{\epsilon}) R_c + (\epsilon_1 - \epsilon_2) \frac{R^3}{R_c^2} \right] + O(\omega^5),$$

$$E_1^{(s)} \approx \frac{1}{3(2\pi)^2} \frac{\omega^2}{c^2} \epsilon_1 R^3 + O(\omega^3),$$

$$E_2^{(s)} \approx \frac{1}{3(2\pi)^2} \frac{\omega^2}{c^2} \epsilon_2 (R_c^3 - R^3) + O(\omega^3),$$

$$\bar{E}^{(s)} = \frac{1}{3(2\pi)^2} \frac{\omega^2}{c^2} \bar{\epsilon} R_c^3.$$

Consequently, we have that

$$\bar{\epsilon} = f\epsilon_1 + (1-f)\epsilon_2.$$

For this value of $\bar{\epsilon}$ it is obviously

$$\text{Re}(\Sigma) \approx 4\pi n \text{Re}(-iD_0/\bar{k}) \approx 0 + O(\omega^4),$$

and, therefore, our final result for the long-wavelength limit in the scalar case is [cf. Eq. (9) and Eq. (4)]

$$\epsilon_\infty = \bar{\epsilon} = f\epsilon_1 + (1-f)\epsilon_2, \quad (10)$$

which is the well-known volume-averaged dielectric constant result. A similar analysis may be carried out for the more complicated vector case. If we, again, abbreviate the right-hand side of Eq. (1) by $\bar{E}^{(v)}$, we find to leading order in ω that only the E field contributes:

$$E_1^{(v)} = \frac{2}{3} \frac{\omega^2}{c^2} \epsilon_1 |d_1|^2 R^3 + O(\omega^3),$$

$$E_2^{(v)} = \frac{1}{3} \frac{\omega^2}{c^2} \epsilon_2 |d_1|^2 \left[2\gamma_1^2 (R_c^3 - R^3) - 9\eta_1^2 \frac{1}{k_2^6} \left(\frac{1}{R_c^3} - \frac{1}{R^3} \right) \right] + O(\omega^3),$$

$$\bar{E}^{(v)} = \frac{2}{3} \frac{\omega^2}{c^2} \bar{\epsilon} R_c^3,$$

where we have the following expansions for the scattering coefficients:

$$d_1 \approx \frac{9\epsilon_2 \bar{\epsilon}}{(2\epsilon_2 + \epsilon_1)(2\bar{\epsilon} + \epsilon_2) + 2f(\epsilon_2 - \epsilon_1)(\bar{\epsilon} - \epsilon_2)} + O(\omega^2),$$

$$\gamma_1 \approx \frac{1}{3} \left(2 + \frac{\epsilon_1}{\epsilon_2} \right) + O(\omega^2),$$

$$\eta_1 \approx \frac{2}{9} (\epsilon_2 - \epsilon_1) \frac{k_2^3}{\epsilon_2} R^3 + O(\omega^6),$$

$$A_1 \approx 2i \frac{\omega^3}{c^3} \sqrt{\bar{\epsilon}^3} \frac{(2\epsilon_2 + \epsilon_1)(\epsilon_2 - \bar{\epsilon})R_c^3 + (\epsilon_1 - \epsilon_2)(\bar{\epsilon} + 2\epsilon_2)R^3}{(2\epsilon_2 + \epsilon_1)(2\bar{\epsilon} + \epsilon_2) + 2f(\epsilon_2 - \epsilon_1)(\bar{\epsilon} - \epsilon_2)} + O(\omega^5),$$

$$B_1 \approx O(\omega^5).$$

Inserting these expressions into Eq. (1) results in a quadratic equation for $\bar{\epsilon}$ which has only one physical solution

$$\bar{\epsilon} = \epsilon_2 \left(1 + \frac{3f\alpha}{1-f\alpha} \right),$$

$$\alpha = \frac{\epsilon_1 - \epsilon_2}{\epsilon_1 + 2\epsilon_2}.$$

Again, just like in the scalar case, it is this particular value for $\bar{\epsilon}$ which makes $\text{Re}(\Sigma)$ vanish up to order $O(\omega^4)$ as can be seen from the expression for A_1 ,

$$\text{Re}(\Sigma) = 4\pi n \text{Re}(-i(A_1 + B_1)/\bar{k}) = 0 + O(\omega^4),$$

so that the final result for the long-wavelength dielectric constant in the vector case is the well-known Maxwell-Garnett result

$$\epsilon_\infty = \bar{\epsilon} = \epsilon_2 \left(1 + \frac{3f\alpha}{1-f\alpha} \right), \quad (11)$$

$$\alpha = \frac{\epsilon_1 - \epsilon_2}{\epsilon_1 + 2\epsilon_2}.$$

Therefore, for both scalar and vector classical waves our mean-field approach gives analytically the correct long-wavelength limit for all values of the filling factor. This is certainly a clear advantage over the theory of Albada *et al.*² who obtained the correct value Eq. (11) only in the limit $f \rightarrow 0$ as well as over our previous approaches^{10,11} which obtained excellent agreement with Eq. (11) for all f only numerically.

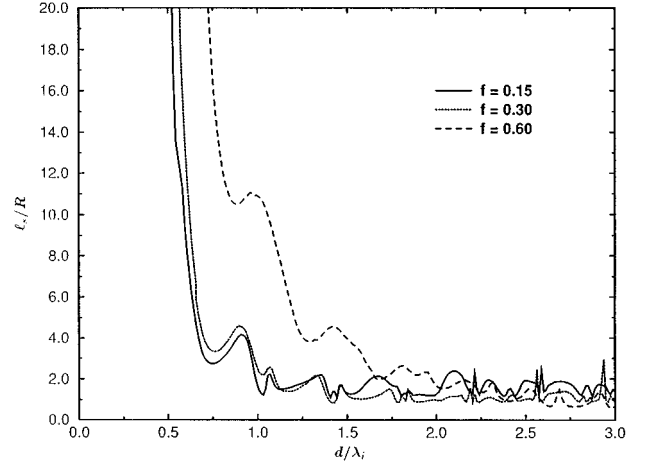


FIG. 2. The scattering mean free path ℓ_s for scalar waves, calculated by the effective medium theory versus d/λ_i for alumina spheres with dielectric constant $\epsilon_1=9$ in vacuum ($\epsilon_2=1$) for different values of the filling factor f .

IV. FINITE FREQUENCIES

For finite frequencies, of course, no analytical solution of Eq. (1) is possible. Fortunately, it turns out that Eq. (1) is numerically much easier to deal with than the self-consistency equations of our previous approaches.^{10,11} To obtain a converged result, we used a simple fixed-point iteration with the long-wavelength limit as a starting value for $\bar{\epsilon}$. The convergence (relative change of $\bar{\epsilon}$ from one iteration step to the next being less than 10^{-4}) was obtained in almost all cases with less than ten iterations. After a successful convergence for $\bar{\epsilon}$ we compute the self-energy Σ according to Eq. (6) and then evaluate Eq. (4) and Eq. (5) for the energy transport velocity v_E and the mean free path ℓ_s , respectively. We chose to present these results for v_E and ℓ_s as a function of d/λ_i , where d is the diameter of the dielectric spheres and $\lambda_i = 2\pi c/\omega\sqrt{\epsilon_1}$ is the wavelength inside the sphere. The reason behind that being the fact that strong Mie resonances of the isolated sphere appear in the limit $\epsilon_1/\epsilon_2 \rightarrow \infty$ when $d/\lambda_i = (n+1)/2$, with $n=1,2,3 \dots$ for the vector and $n=0,1,2, \dots$ for the scalar case. Furthermore, it should be noted that we used different numbers of scattering coefficients in the series given by $E^{(s)}$ and $E^{(v)}$. We found that increasing the maximal number of scattering coefficients beyond 10 does not alter the results in the range of d/λ_i which we have considered.

Figures 2 and 3 show the scattering mean free path ℓ_s in units of the sphere radius R for scalar and vector classical waves, respectively, versus d/λ_i for the experimental setup of Garcia *et al.*,⁹ which consisted of a mixture of alumina spheres with dielectric constant $\epsilon_1=9$ and hollow polypropylene spheres $\epsilon_2 \approx 1$, for different values of the filling factor f of the alumina spheres. Figures showing the energy transport velocity v_E for scalar and vector classical waves, respectively, versus d/λ_i for the same configurations can be found in Ref. 12. It can be clearly seen that for low values of the filling factor v_E exhibits large dips near the Mie resonances which become smeared out as the filling factor increases. This displays the fact that due to the multiple scattering contributions the effective medium gets stronger

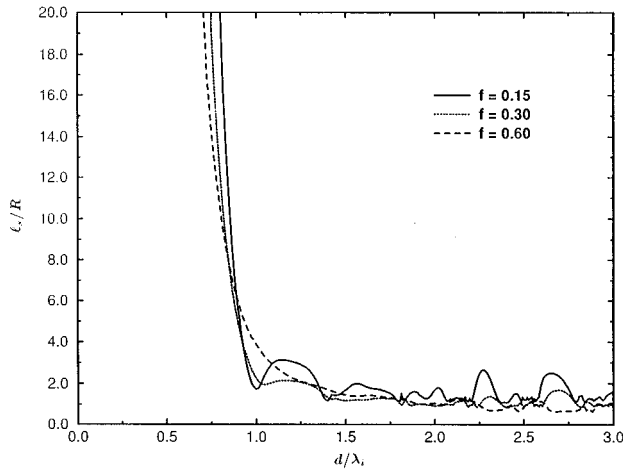


FIG. 3. The scattering mean free path ℓ_s for vector waves, calculated by the effective medium theory versus d/λ_i for alumina spheres with dielectric constant $\epsilon_1=9$ in vacuum ($\epsilon_2=1$) for different values of the filling factor f .

renormalized as f increases, thus competing with the single-scatterer effects which dominate at low filling factors f . This qualitative behavior has been confirmed by experiment.⁹

To further check the effective medium scheme we compare it with recent experiments of Garcia *et al.*⁹ They have measured the frequency dependence of microwave propagation in a sample of 1/2-in. polystyrene spheres with index of refraction 1.59 and filling ratio of $f=0.59$. Their experimental results (solid circles) as well as the results of our effective medium theory (crosses) are presented in Figs. 4, 5, and 6, where the frequency dependences of the diffusion coefficient $D=v_E\ell_s/3$, transport velocity v_E and mean free path ℓ_s are shown. The relation between experimental frequency ν and d/λ_i is, in this case, ν (GHz) ≈ 15 (d/λ_i). The parameters used in the theoretical calculations are $\epsilon_1=2.53$, $\epsilon_2=1$, $f=0.59$, and $R=0.64$ cm. It is evident that there is rather

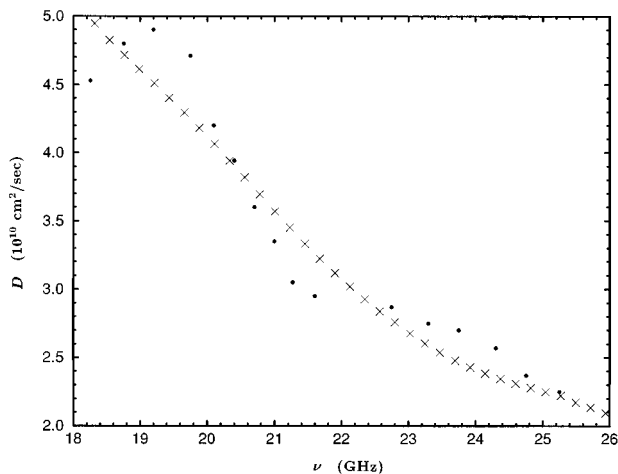


FIG. 4. The frequency dependence of the diffusion constant for a sample of 1/2-in. polystyrene spheres with index of refraction 1.59 and filling ratio 59%. The solid circles correspond to the experimental values whereas the crosses are the results of the effective medium theory.

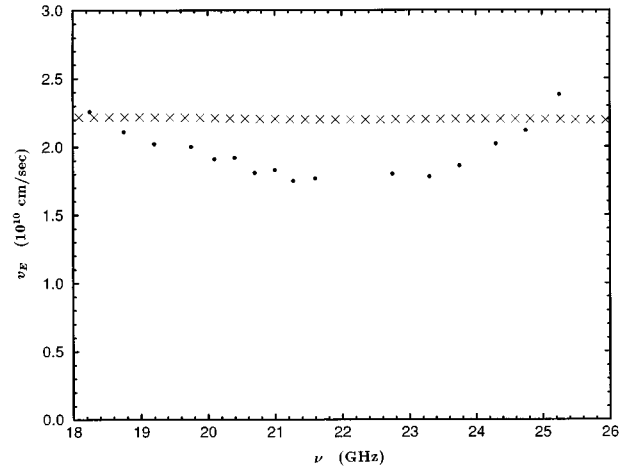


FIG. 5. The frequency dependence of the energy transport velocity for a sample of 1/2-in. polystyrene spheres with index of refraction 1.59 and filling ratio 59%. The solid circles correspond to the experimental values whereas the crosses are the results of the effective medium theory.

good agreement between the experimental and theoretical results, both in magnitude and overall frequency dependence. However, v_E is flatter than the experimental one. As for the comparison of the experimental mean free path and the effective medium result, Fig. 6, there is indeed a semiquantitative agreement for $\nu \geq 19$ GHz but the experimental drop in low frequencies is very difficult to understand theoretically.

V. DISCUSSION

In summary, we have presented a scheme for calculating the transport properties of random media. This scheme captures the effects of Mie resonances, always present in cases of finite scatterers, exactly and the multiple scattering contributions in a mean-field sense. It is proposed that the choice of an effective medium is based on the principle that the

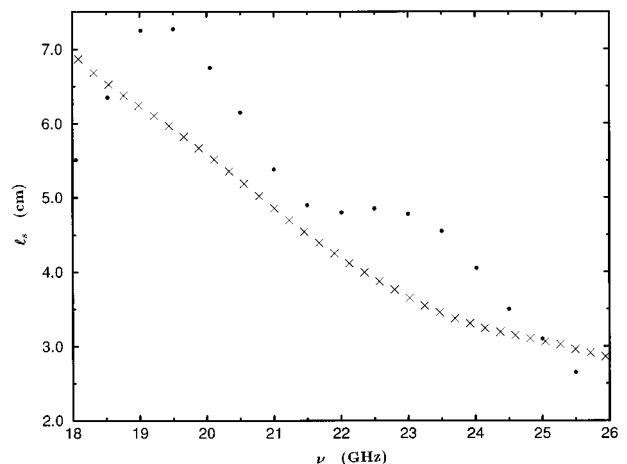


FIG. 6. The frequency dependence of the scattering mean free path for a sample of 1/2-in. polystyrene spheres with index of refraction 1.59 and filling ratio 59%. The solid circles correspond to the experimental values whereas the crosses are the results of the effective medium theory.

wave energy density should be uniform when averaged over length scales larger than the size of the inhomogeneities. We have applied this effective medium theory to scalar and vector waves. In both cases a careful analysis of the long-wavelength limit rediscovers the well-known results. For finite frequencies the computational effort as compared to approaches based on an average TCS (Refs. 10,11) is greatly reduced and there have been no convergence problems for all parameters which we considered. In addition, the theory contains no adjustable parameter. The results for the scattering mean free path ℓ_s are consistent with the excellent results that have been obtained with the aforementioned approaches.^{10,11} Furthermore, the theory obtains values for the energy transport velocity v_E that are consistent with experimental values for all filling factors f , thus bridging the gap between the low-density theory of Albada *et al.*² and the high-density results of Refs. 10,11 in a very natural way. This scheme can be easily applied to different types of clas-

sical waves. In particular, the application of this method to elastic wave will be very interesting, since for this case no theory exists as yet.

ACKNOWLEDGMENTS

We want to thank Ping Sheng for discussing an energy homogenization idea as applied to the scalar wave case in Chap. 8 of his book,¹⁴ and E. N. Economou, J. Kroha, and P. Wölfle for useful discussions. Ames Laboratory is operated for the U.S. Department of Energy by Iowa State University under Contract No. W-7405-ENG-82. This work was supported by the Director of Energy Research, Office of Basic Energy Sciences and NATO Grant No. CRG 940647. K.B. acknowledges support by the Sonderforschungsbereich 195, "Lokalisierung von Elektronen in makroskopischen und mikroskopischen Systemen" at the University of Karlsruhe.

¹For a review, see *Scattering and Localization of Classical Waves in Random Media*, edited by Ping Sheng (World Scientific, Singapore, 1990); *Photonic Band Gaps and Localization*, edited by C. M. Soukoulis (Plenum, New York, 1993).

²M. P. van Albada, B. A. van Tiggelen, A. Lagendijk, and A. Tip, Phys. Rev. Lett. **66**, 3132 (1991); Phys. Rev. B **45**, 12233 (1992).

³J. Kroha, C. M. Soukoulis, and P. Wölfle, Phys. Rev. B **47**, 11093 (1993).

⁴E. Kogan and M. Kaveh, Phys. Rev. B **46**, 10636 (1992).

⁵G. Cwilich and Y. Fu, Phys. Rev. B **46**, 12015 (1992).

⁶Yu. N. Barabanenkov and V. Ozrin, Phys. Rev. Lett. **69**, 1364 (1992).

⁷B. A. van Tiggelen, A. Lagendijk, and A. Tip, Phys. Rev. Lett. **71**, 1284 (1993).

⁸B. A. van Tiggelen and A. Lagendijk, Europhys. Lett. **23**, 311 (1993).

⁹N. Garcia, A. Z. Genack, and A. A. Lisyansky, Phys. Rev. B **46**, 14475 (1992); A. A. Lisyansky *et al.*, in *Photonic Band Gaps*

and Localization, edited by C. M. Soukoulis (Plenum, New York, 1993), p. 171.

¹⁰C. M. Soukoulis, S. Datta, and E. N. Economou, Phys. Rev. B **49**, 3800 (1994).

¹¹K. Busch, C. M. Soukoulis, and E. N. Economou, Phys. Rev. B **50**, 93 (1994).

¹²K. Busch and C. M. Soukoulis, Phys. Rev. Lett. **75**, 3442 (1995).

¹³A. Gonis, *Green Functions for Ordered and Disordered Systems* (North-Holland, New York, 1992).

¹⁴Ping Sheng, *Introduction to Wave Scattering, Localization and Mesoscopic Phenomena* (Academic, New York, 1995), Chaps. 3, 4, and 8.

¹⁵X. Jing, P. Sheng, and M. Zhou, Phys. Rev. A **46**, 6513 (1992); Physica A **207**, 37 (1994).

¹⁶C. F. Bohren and D. R. Huffman, *Absorption and Scattering of Light by Small Particles* (Wiley Interscience, New York, 1983).

¹⁷D. A. G. Brüggeman, Ann. Phys. (N.Y.) **24**, 636 (1935).

¹⁸J. C. Maxwell-Garnett, Philos. Trans. R. Soc. London A **203**, 385 (1904).

¹⁹D. J. Bergman, Ann. Phys. (N.Y.) **138**, 78 (1982).